REPORT

OF

PORT AND HARBOUR TECHNICAL RESEARCH INSTITUTE

REPORT NO. 5

Wind Wave in Decay Area

by

Hisashi Mitsuyasu

Hisao Kimura

April 1964

PORT AND HARBOUR TECHNICAL RESEARCH INSTITUTE

MINISTRY OF TRANSPORTATION

162 Kawama Yokosuka-City Kanagawa-Prefecture, Japan

CONTENTS

WIND WAVE IN DECAY AREA

Abstract

Measurements of wind waves have been done in the decay area of large scale wind flume (70 m × 1.5 m × 1.3 m) including a point at the end of generating area, and one-dimensional wave spectrum have been studied associated with the analysis of wave properties obtained directly from the wave record. As the propagation of the wind wave in decay area gradual increase of mean wave period was found associated with the decrease of mean wave height, and such changes of mean wave properties were closely related to the decay of wave spectrum.

The Gaussian hypothesis of wind wave was not particularly substantiated in the generating area nor in the initial part of the decay area. However, as the propagation of the waves in decay area and as the decrease of nonlinearity of wave the frequency distribution approached gradually to the Gaussian distribution.

When the wave propagated into the decay area, short ripples generated by wind shear damped out quickly. But carefull observation revealed the existence of tiny ripples near the crest of dominant waves even at the decay area far from the generating area. Those ripples were considered to be generated by the mechanisum studid by Longuet-Higgins (1963).

Wave spectrum in decay area showed interesting characteristics. Conspicuous energy transfer from high frequency to low frequency was observed near the dominant peak of the spectrum especially when the wave was breaking at the initial part of the decay area. The dissipation of the wave energy at high frequency part was very close to that due to molecular viscosity but dissipation of energy much greater than that due to molecular viscosity was observed near the dominant peak on the spectrum.

Due to the narrow band width of wave spectum, the second peak due to nonlinear effect appeared to almost highest frequency part of our spectrum. So the equilibrium range in a strict meaning could not be observed. However, the form of spectrum was fairly close to the universal form proposed by Kitaigorodski except for the excess energy concentrated near the dominant peak and the second peak at nearly twice of the frequency of dominant peak.

Second peak has disappeard gradually as the propagation of wave in decay area. Excess energy near the dominant peak also decreased gradually in the decay area; some of them seemed to be transferred to low frequency range by breaking of wave and some of them seemed to be dissipated by complicated mechanisum wich we have few knowledge about.

§ 1. Introduction

In the last decade, great many theoretical and observational studies of wind waves have been conducted and still now they are continuing. The generation of waves by wind, development of waves due to wind action, statistical properties

of ocean waves, and non-linear interaction of random waves, such basic problems have been vigorously studied in many countries associated with the study of waves of synthetic aspect such as wave forecasting.

However, as far as we know, there are few quantitative data about the decay of wind waves, except for several theoretical treaments of this problem [Sverdrup & Munk (1947), Barber & Ursell (1948), Grone & Dorestein (1950)]. This problem is not only interesting from the theoretical standpoint but also very important for the explanation of the generation of swell.

This paper is mainly concerned with the decay of wind waves which are generated in the wave tank by wind blower and propagate into the calm area. In such a laboratory study we can treat the problem in much simplified conditions.

In the ocean, unsteadiness of generated waves, angular spreading and discrimination of wind waves in decay area, viscosity of water (molecular and turbulence), air resistance, ocean current, local wind in decay area, interaction of the swell with the locally generated wind waves and geographic condition of the observation station, such great many factors will affect the decay of wind waves. Therefore, it demands very carefully planned observation of tremendous large scale to obtain the reliable data, and it will be difficult to analyze the data and to evaluate the effect of individual factor.

In the laboratory we can study systematically what is happening in the decay area of wind wave. This has been the intention of the commencement of this study. However, several problems will arise in the laboratory study too. Due to the short limited fetch of the wave tank, the band width of wave spectrum is not so wide and limited to fairly high frequency range. Therefore, the importance of the different terms in the dissipation mechanism of wave energy is slightly different from that in actual ocean waves which contain the as much amount of energy in lower frequency as compared to the waves generated in the tank. The existence of side wall of the wave tank will also affect the properties of wind waves because the propagating direction of wind waves is much limited by the side wall. We must be careful of such points when we discuss the actual ocean waves by comparing with the present experimental results.

The discussions will be mainly devoted to the statistical properties of wind waves in decay area such as Gaussian property, and to the decay of wave spectrum.

§2. Experimental Arrangement and Techniques

2–1. Wind flume and experimental procedures

The experiments were conducted in the large scale wind flume which was constructed recently in the hydraulic laboratory of Port and Harbour Technical

Research Institute to study the following various problems:

(i) Generation and development of wind waves
(ii) Decay of wind waves
(iii) Wind wave action against a structure
(iv) Interactions between waves and currents
(v) Wind shear stress and water surface roughness.

To apply to these various kinds of studies, this flume has a special shape and scale shown in Figure 1 and has the following equipment and characteristics:

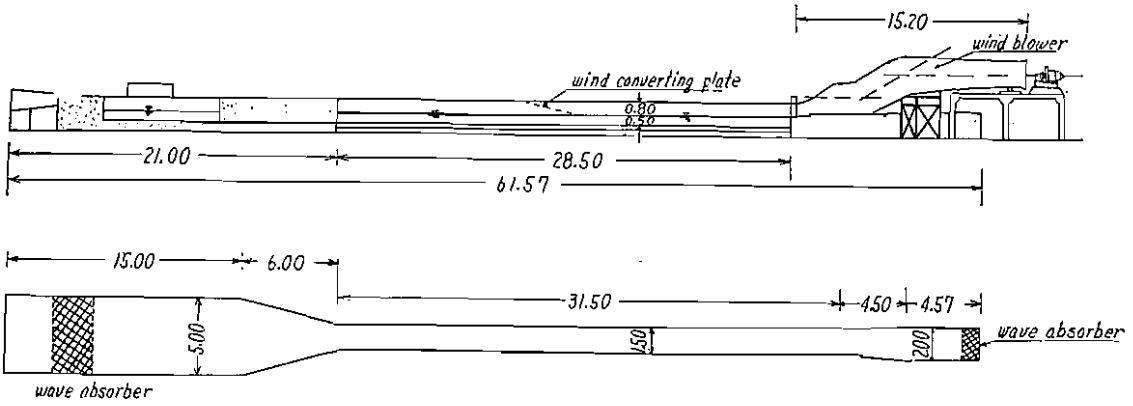

Fig.-1. Wind Flume (unit: m)

(1) Wind blower (centrifugal) 75 HP, mean wind speed 3–30 m/sec (variable)
(ii) Wave generator (piston type), pericd 1–4 sec, max. wave height 25 cm.
(iii) Tide generator (pneumatic type), pericd 7 min. or greater, max. amplitude ±10 cm. arbitrary wave form can be generated by automatic control system.

Careful attention has been paid to maintain a uniform velocity and low turbulence wind* at the inlet of the wind flume. Although intensity of turbulence was not measured yet, the velocity distribution of wind was almost uniform at the inlet.

The present studies were conducted by using only a wind blower throughout the experiment, water depth was 50 cm. and two kinds of wind speed,

$$\bar{u}=8.12 \text{ m/sec.} \qquad \bar{u}=10.80 \text{ m/sec.},$$

$$\text{rpm}=300 \qquad \text{rpm}=400$$

were used to generate wind waves. rpm indicates the rotation of blower's propeller per minute, and hereafter we specify the experimental cases by the number of rpm, i. e., rpm=300 and rpm=400. At the middle part of the tank, about 13 m from

* Some modification of wind profile or turbulence intensity is possible by replacing the fine mesh net with another coarse grid or special apparatus to give the disturbance for the wind.

the inlet, air flow was converted to the outside of the flume by inserting a sloped plate. Therefore, the area between the inlet and this point in the flume corresponds to the generating area, and the area between this point and the end of the flume where the wave absorber is inserted corresponds to the decay area. As shown in Figure 1, the rear part of the flume was widened from 1.5 m to 5.0 m. The wave energy was spread and finally absorbed effectively by the wave absorber. Therefore, reflected waves were negligible.

Waves were measured by using parallel wire resistance elements at the several points on the center line of the flume. Measured positions of the waves were shown schematically in Figure 2. Actually, however, simultaneous measurements were confined only to two points always including No. 1 point. Waves

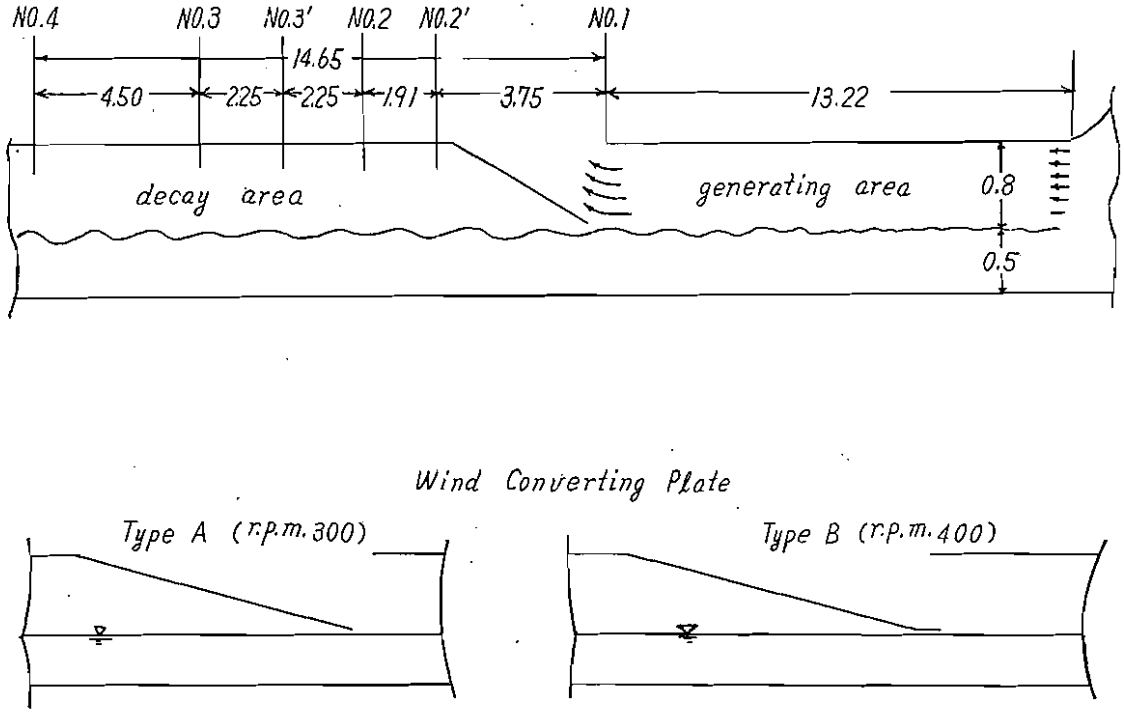

Fig.-2. Measuring Position and Wind Converting Plate (unit: m)

were recorded on a chart recorder and one of these waves was recorded simultaneously on magnetic tape. Due to the restriction of the tape tracks, simultaneous recording of waves on the tape, which is ideal, was impossible. Therefore, much attetion was paid to maintaining the same experimental conditions in each case when the measurement of the same series, but of different measuring points, was conducted. That is, rotation of the wind blower was adjusted carefully to produce the same wind velocities each time; the measurements were begun in each case 10 minutes after the wind blower was started (a sufficient time to

attain a steady condition of wind waves); the measurements of each series (i. e., same r.p.m.) were conducted within the same day to reduce change of conditions as much as possible; finally the experimental conditions were checked by using the chart record which always included the wave record at No. 1 position which corresponds to the end point of the generating area. The variations of mean wave properties at the order of one percent were found from the records measured at No. 1 position at different times. But corrections by using this variation of initial condition of the wave properties were not conducted.

2-2. Wave measuring instrument

Waves were measured by using parallel wire resistance elements. The main characteristics of this instrument is as follows:

(i) Diameter of the wire (gold coated Cu-Pb wire) 0.5 mm
(ii) Clearance between wires 20 mm (at bottom), 10 mm (at top)
(iii) Hysterisis of the total measuring system 2%
(iv) Variation of the sensitivity 1%/hour
(v) Linearity within 1%

The waves were recorded simultaneously on a chart recorder and low speed tape recorder. Figure 3 shows the block diagram of the measuring system of waves.

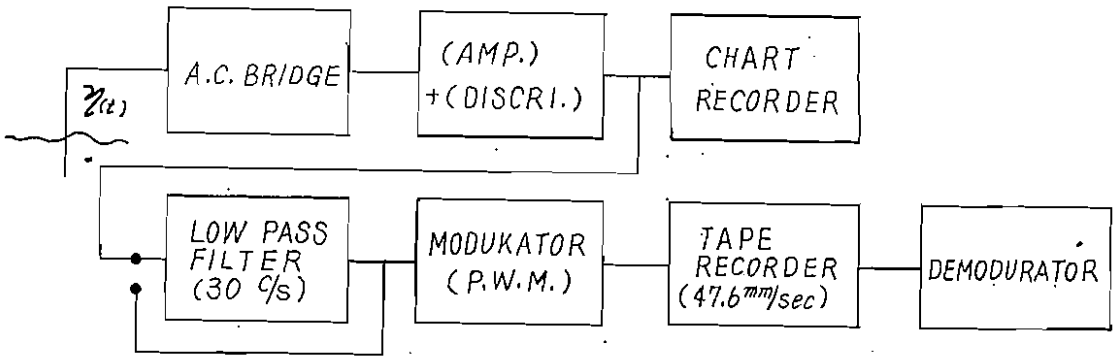

Fig.-3. Wave Measuring Instrument

Although exact response characteristics were difficult to determine, it was found that this wave measuring system could detect the ripple of about 8 c/s. It was estimated that response characteristics would be sufficient to detect the short wind wave which has a frequency lower than about 5 c/s.

The characteristics of the tape recorder was listed in Table 1, and the frequency responce of chart recorder was almost flat from 0 to 10 c/s. As far as frequency response is concerned that of the recorder is sufficiently enough as compared to the response characteristics of the staff itself.

TABLE 1.

Data Recorder (Low Speed Tape Recorder)

Modullation	P.W.M (Calier ; 200 C/S)
Tape Speed	47.6mm/sec
Deviation of Speed	±0.5%
Wow and Flutter	±0.5%
Frequency Response	0~20 C/S (under ±1db)
Linearity	3%
S/N Ratio	40 db.
Drift	Within 1%
Input Filter	30 C/S Low Pass Filter

2-3. Wave spectrum analyzer

The wave spectrum analyzer is an analog type analyzer which is similar to that of Chan's (1954) one except for slight differences in the detailed structure and characteristics. That is, the analyzer was composed of three parts; a high

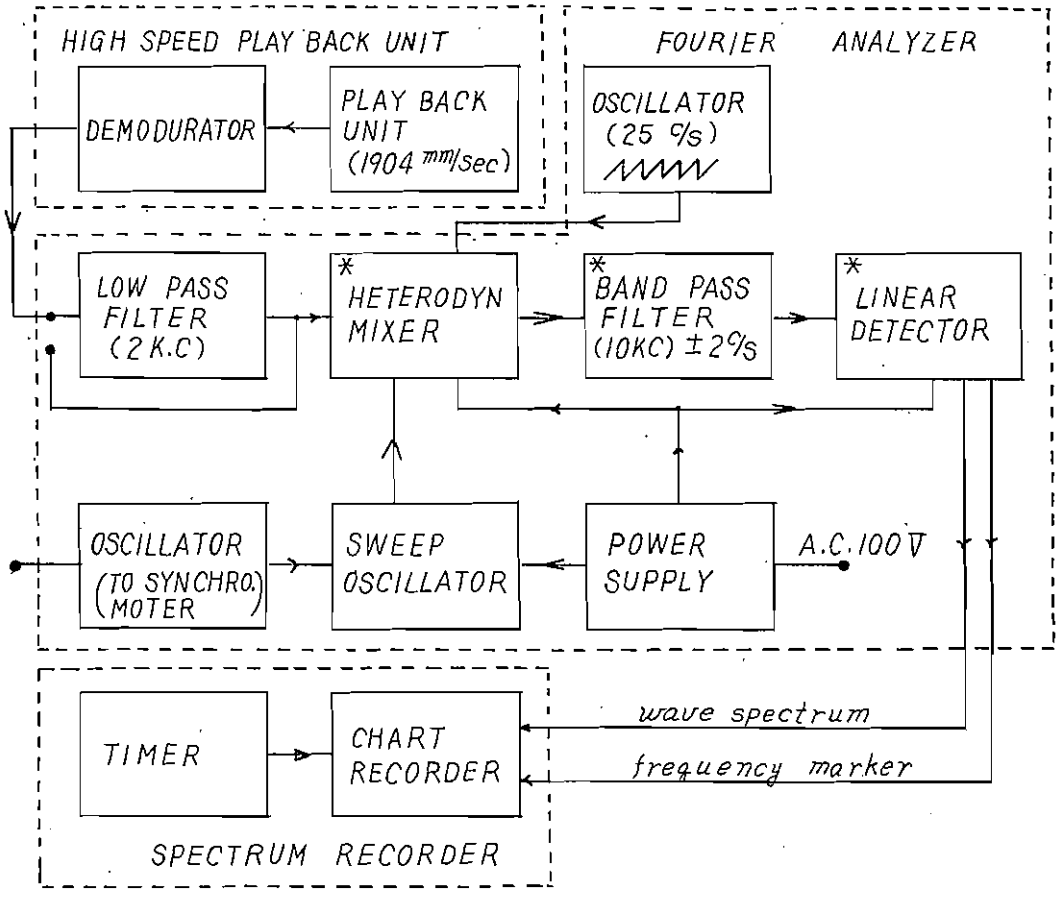

(* TWO SETS)

Fig.-4. Wave Spectrum Analyzer

speed playback unit with demodurator; heterodyne type Fourier analyzer with linear detector; and a pen recorder with D. C. amplifier. The block diagram of the analyzer was shown in Figure 4.

When this analyzer was designed mcuh careful attention was paid to the increase of accuracy of frequency in the measuring system (which is relatively difficult as compared to the increase in accuracy of amplitude). For this purpose the following two special methods were adopted:

(i) To obtain a uniform frequency change of the sweep oscillator the air condenser which was carefully manufactured was driven by the synchronous motor operated by the crystal oscillator of accurate frequency;

(ii) At the same time of the spectrum analysis of wind wave the sawtooth wave of 25 c/s generated by the crystal oscillator was analyzed and their harmonics were used as the frequency markers.

Instead of the square law detector, the linear detector was adopted to increase the accuracy of the spectrum in high frequency range. Becacause at the high frequency range of the spectrum wave energy is very small as compared to that of dominant part, the analyzer is required to have much wider dynamic range. By using the linlar detector we can record more uniform spectrum than that obtained by square law detector. This saves the decrease of the accuracy of the spectrum measurement in high frequency range. Therefore, the amplitude of the recorded spectrum was squared by using a calculator to obtain the power spectrum. Various characteristics of the spectrum analyzer were listed in Table 2, Table 3 and Table 4.

TABLE 2.

High Speed Playback Unit

Tape Speed	1905mm/sec (47.6 mm/sec × 40)
Length of Endless Tape*	2m~9m
Frequency Response	0~800 C/S (±1db)
Total Harmonic Distortion	2% (at 200 C/S)
S/N Ratio	40 db
Drift	Within 1%

* 5.71m tape was used in the present analysis

During the preliminary test of the analyzer some difficulties were found: (i) linearity of the detector is not so good, espectially when the signal and therefore, the output of the analyzer is very small. This is caused by the fundamental characteristics of the vacume tube for which it is difficult to have an ideal linearity. So calibration curves were made corresponding to several definite sensitivities of the analyzer and the measured spectrum were finally corrected by using these

TABLE 3.

Chart Recorder of Spectrum Analyzer

Chart Width	60 mm
Gain (D. C. amp.)	50 db. (max.)
Linearity (including pen)	2 %
Frequency Response	0~10 C/S (Within ±5%)
Noise (at maximum gain)	Less than 0.3mm
Drift	Less than 0.6 mm/hour

TABLE 4.

Fourier Analyzer (Heterodyne Type)

Frequency Range*	10~800 C/S (0.5~20 C/S; corresponding input frequency
Frequency Response	10~800 C/S Within 0.2 db.
Sweep Oscillator	10000~9200 C/S (accuracy 10^{-4})
Sweep Velocity	1/2 C/S / sec or 1/3 C/S / sec (accuracy ±0.5%)
Frequency Marker	25 C/S interval (0~200 C/S) 50 C/S interval (200~800 C/S) accuracy ± 1 C/S
Band Pass Filter** (Crystal)	No.1 Center Frequency 10 KC (2×10^{-5}) Band Width ± 1 C/S 40 db. down at ±12C/S No.2 Center Frequency 10 KC (2×10^{-5}) Band Width ± 2 C/S 40 db. down at ±18C/S Effective Band Width 4.95 C/S (used)

* It must be care that frequencies dealt in this table were increased 40 times greater than the frequency in the actual phenomena due to the increased reproducing tape speed 40 times greater than the recording tape speed.

** Band Pass Filter No. 2 was used in the present study.

calibration curves. (ii) to eliminate the zig zag form in recorded spectrum due to the variation of the instantaneous intensity of wave spectrum averaging circuit which has a time constant of about 3 seconds was inserted between the analyzer and chart recorder. This Time constant was comparable to a period of rotation of the tape loop and was most adequate.

2-4 Calibration of wave staff and spectrum analyzer

Before and after the measurement of waves was condncted wave staff was calibrated by inserting the staff by the definite amount and recording the output on the chart recorder.

Even by a slight oil film on the water surface the sensitivity of wave staff was greatly changed. So much care was paid to keep the water clean.

The spectrum analyzer was calibrated by using a method similar to that of Marks (1960), Pieson (1954) or Chang (1954). That is, calibration of the amplitude, frequency and filter were made by using a oscillator and applying the simple sine wave of known voltage and frequency.

Fourier analyzer had a self-calibrating system in which the output of the crystal oscillator of 50c/s and of definite magnitude was analyzed and indicated in the panel meter.

Pen recorder had also a self-calibrating system in which the definite D-C voltage was supplied to the input.

The calibration of the total analyzing system was practiced by using a test tape in which the definite signal (frequency and intensity) was recorded. However, this calibration was practiced only twice in a daily measurement, i. e., before and after the series of measurement, due to the good stability of analyzing system.

Partial calibrations by using the self contained calibration system were made every time when each individual analysis was practiced.

2-5 Confidence limit of the measured wave spectrum

The confidence bands were determined from the chi-squared distribution with f degree of freedom where

$$f=2T\Delta f\,.$$

T is the time it takes the magnetic tape loop to make one traverse through the analyzer ($T=3$ sec. in our case), Δf is the effeclive band width of the filter ($\Delta f=4.95$ c/s in our case) and therefore, $f\fallingdotseq 30$.

As the three independent tape loops were used to obtain a spectrum of the same series of experiment and their mean values were used, total degree of freedom of the spectrum density becomes

$$f\fallingdotseq 90\,.$$

The corresponding multiplication factors for the spectrum to obtain the 90% confidence limit become

1.31 and 0.80.

§ 3. Wind Wave in Decay Area

3-1 General properties of wind waves in decay area

The observation of wind wave were conducted in a decaying area in which the waves were stationary propagating from generating area to the end of the tank and the wind was never blowing over the water surface. In order to under-

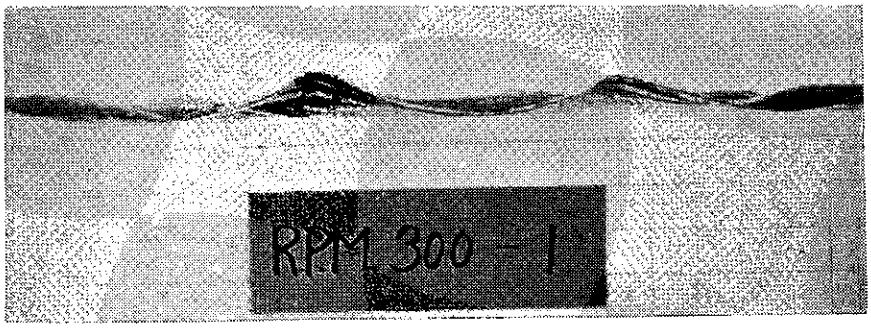

Station No. 1

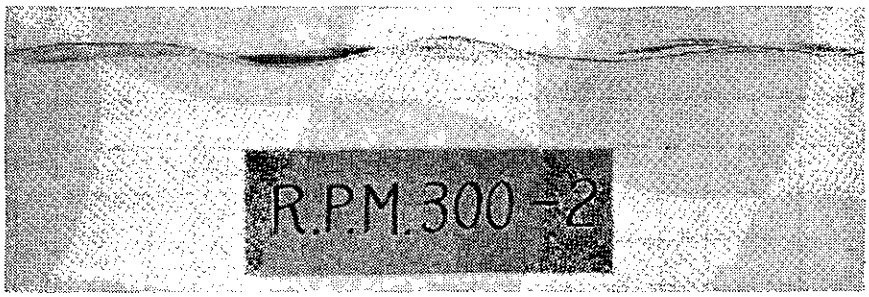

Station No. 2

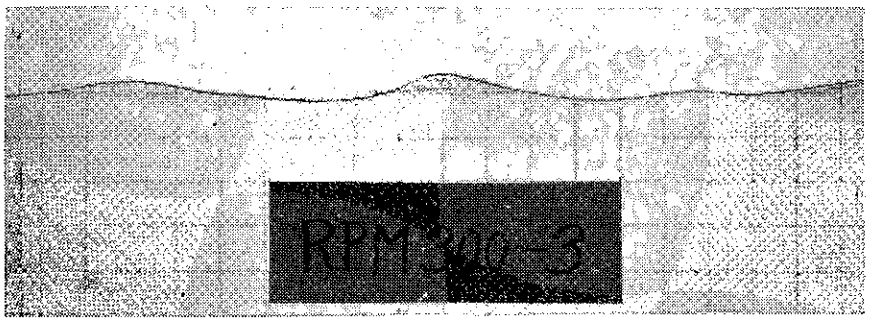

Station No. 3

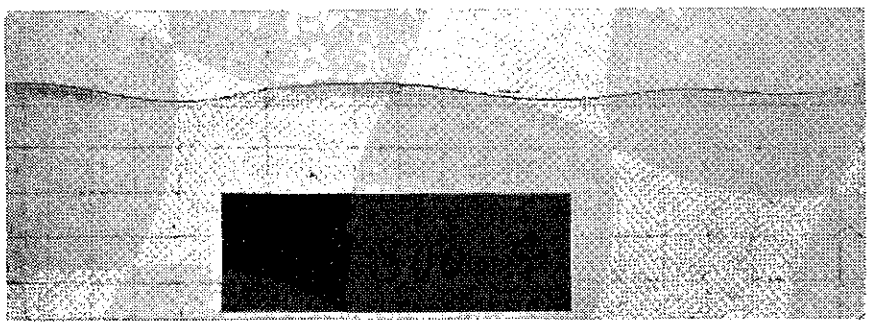

Station No. 4

Fig. 5-a. Wind Wave in Decay Area (r.p.m 300)
Mesh line is 50 mm interval. Direction of wave propagation is from righ to left.

Station No. 1

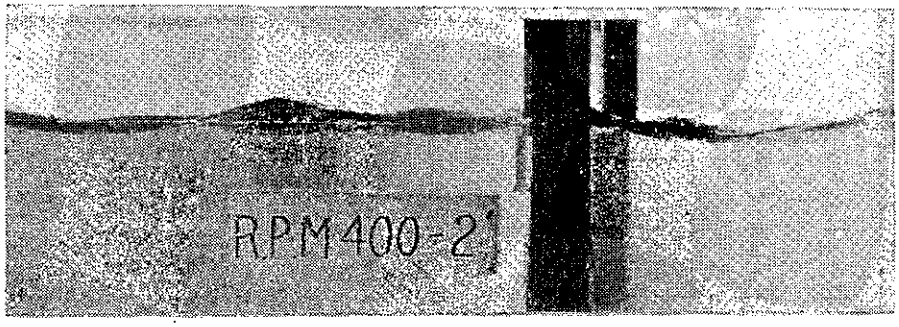

Station No. 2′

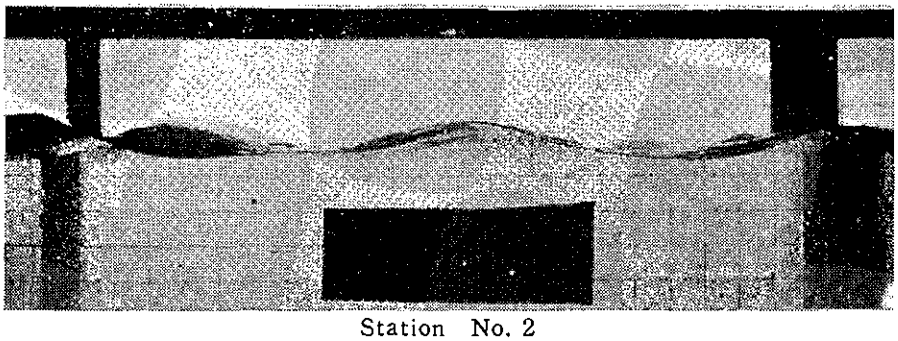

Station No. 2

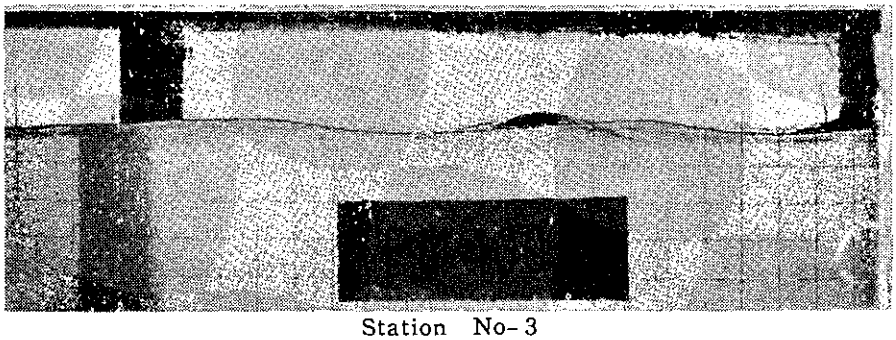

Station No-3

Fig. 5-b. Wind Wave in Decay Area (r. p. m. 400)
Mesh line is 50 mm interval. Direction of wave propagation is from right to left.

stand what was happening in the decaying area visual observation of the waves were first conducted, and the waves were then photographed through the side wall of the flume which was made from glass scaled with mesh line of 50 mm interval. Figure 5 shows photographs of the typical wind waves. Essential properties of wind waves such obtained in various staticns are the followıng:

A. R.P.M. 300 ($\bar{U}$=8.12 m/sec)

Station No. 1 (at the end of generating area)

Wind waves were almost saturated conditions, i. e., the breaking of waves were occuring frequently, and dominant waves were covered with the short ripples. Due to the effect of surface tensicn between the glass wall and water capillary waves overlapping the dominant waves are nct so clear ın the photograph (Figure. 5). However, ripples which covered the dominant wave were clearly observed from the upper window of the flume. Moreover, dominant waves clearly showed the short crestness, i. e., " hexagcnal form ", and their crest lengths were 30-40 cm., 1/5-1/4 of the flume width.

Area between Station No. 1 and Station No. 2

In the range of 1 m from the Station No. 1, waves changed greatly, i. e., the crest of waves broke in many times when they passed under the wind converting plate and were propagated into the calm area. Breaking of small scale were still continued to the position 3 m downward from the Station No. 1, and gradually waves became smooth. As will be discussed in the later section these breaking of waves greatly changed the structure of wave spectrum, and showed the very interesting properties concerning the energy transfer in the spectrum.

Station No. 2

Waves were very smooth and had nearly symmetrical form against the still water level. However, steep waves of large amplitude showed clearly nonlinear properties, i. e., steep crest and flat trough. In some case waves broke near the crest. The careful observation from the upper window of the flume showed that dominant waves were still overlapped with short ripple of very small amplitude.

Station No. 3 and Station No. 4

In these stations waves became gradually smooth and never broke as shown in Figure 5. However, short ripples of very small amplitude were still observed at the frcnt part of the dominant waves.

B. R.P.M. 400 ($\bar{U}$=10.80 m/sec)

Station No. 1

Almost all the waves were continually breaking and dominant waves were covered

with the short ripples. Although forward inclination of the wave crest was not so clear, wave crests were much steeper than the wave trough.

Area Between Station No. 1 and Station No. 2

In the range of 2 m from the Station No. 1 breaking of large scale occured, irregular short ripples covering the dominant waves disappeared, and waves became relatively smooth. However, regular ripples of small amplitude overlapped near the front part of the dominant wave crest, and breaking of waves occured some times when the steep waves were produced by the interaction of the wave components.

A peculiar phenomenon in this case was the increase of wave height when the wave passed through the gap under the wind converting plate. This perhaps was due to the special pressure distribution over the wave surface at the moment when the wave was propagated just under the converting plate. That is, at the backward side of the wave crest strong wind pressure might act, but there were no such strong pressure at the front part. In the case of R.P.M. 300, such a phenomenon was not found. This perhaps was due to the different shape of the wind converting plate. (Figure 2).

Station No. 2

Only a few times waves broke with the slight forward inclination of the crest. Dominant waves were still overlapped with regular short ripples of very small amplitude and had unsymmetrical form against the still water level.

Station No. 3

Nonlinearity of wave was greatly diminished; waves had almost symmetrical forms against the still water level except for the few cases where the waves became steep by the interaction of component waves and finally broke. Tiny ripples overlapped on the front part of the dominant waves.

Station No. 4

Waves became increasingly smooth with breaking occuring only a few times. But overlapping short ripples with very small amplitude still existed.

Summing up:

(1) Aside from the deformation of waves due to the special wind pressure at the moment when the waves pass through the gap under tne wind converting plate, wave changed greatly after travelling 3-4 wave lengths from the generating area to the calm area; i. e., large scale breaking of waves occured frequently, irregular short ripples covered the almost entire surface of dominant waves extinguished, and waves became increasingly smooth.

Such changes of wave properties were also reflected clearly in the change of wave spectrum as shown in the later chapter.

(ii) Even after the waves become very smooth as the propagation in the decay area careful observation showed the overlapping of short ripples near the front part of the dominant wave crest. As such a short ripple should damp out quickly due to the viscosity some special mechanism must exist to maintain it. This seems to be the same phenomenon as that observed by C. S. Cox in his measuremement of wave slope. That is, in his study short ripples overlapped on the dominant waves were measured even when the uniform waves were generated by oscillating paddle without wind.

Recently, Longuett Higgins (1963) discussed this problem theoretically. According to his theory, capillary waves may be generated by at least two mechanisms:

(1) instability in the shearing air-stream as described by Miles (1962), and

(2) by the action of surface tension near the crests of gravity waves.

Capillary waves generated by the second mechanism tend to occur on the forward slopes of gravity waves, from which they may extract appreciable energy. That is, much amount of energy is transferred from dominant wave to short ripples overlapped on it due to nonlinear effect (radiation stress) and the energy is dissipated in the short ripples due to the viscosity. Some of the energy dissipation near the dominant peak of wave spectrum should be attributed to this mechanisum.

3-2 Gaussian Property of Wind Wave

Many of the wind wave theories have been based on the assumption that the surface displacement. $\eta(t)$ of the wind wave can be considered as the realization of Gaussian random process. And this has been proved as a fairly good assumption in a first approximation [Pierson(1952)].

However, we will be able to expect some deviations of actual wave properties from the Gaussian properties when we remember the unsymmetrical wave form of steep wave due to nonlinearity.

Blair Kinsman(1960)made a detailed study of this problem and obtained the results that actual frequency distributions did not correspond particularly well to the Gaussian even when the data were seemingly Gaussian.

Recently Longuet-Higgins(1963)discussed this problem theoretically and derived the statistical density function of Gram-Charlier type in the case of "weakly nonlinear". He also obtained the Gaussian distribution as the first approximation.

To provide further information about this problem each wave record on our chart paper obtained simultaneously with the recording on magnetic tape was analyzed. Sampled values of surface elevation. $\eta(t)$ were sorted out in the interval

of 1/6 secnd (r.p.m. 400) and 1/12 second (r.p.m. 300) from each of the 2 minute wave records*, and their mean square values, root mean square vaues and frequency distributions were obtained.

Figure 6 - Figure 7 show the frequency distributions of our sorted values of the surface elevations and the corresponding Gaussian distribution curves. And Table-5 shows the values of various quantities relating to the statistical distribution, i. e., moments (μ_2, μ_3, μ_4), skewness ($\sqrt{\beta_1}=\mu_3/\mu_2^{3/2}$), kurtosis ($\beta_2=\mu_4/\mu_2^2$), the value of chi-square and associated probability calculated on the assumption that they are random samples from Gaussian process.**

Visually the data fit the Gaussian distributions fairly well, but χ^2-test and the values of skewness and kurtosis show coincidence being not particularly well. Especially at the generating area (Station No.1), and moreover, in the case of r.p.m. 400, deviation from the Gaussian is conspicuous. This should reflect that the wave steepness and therefore, the nonlinearity was highest in this case among

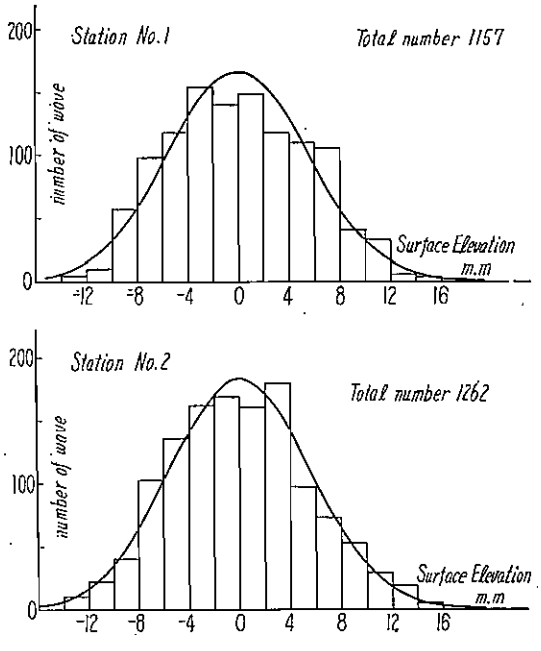

Fig 6-a. Histogram of Surface Elevation (r.p.m 300)

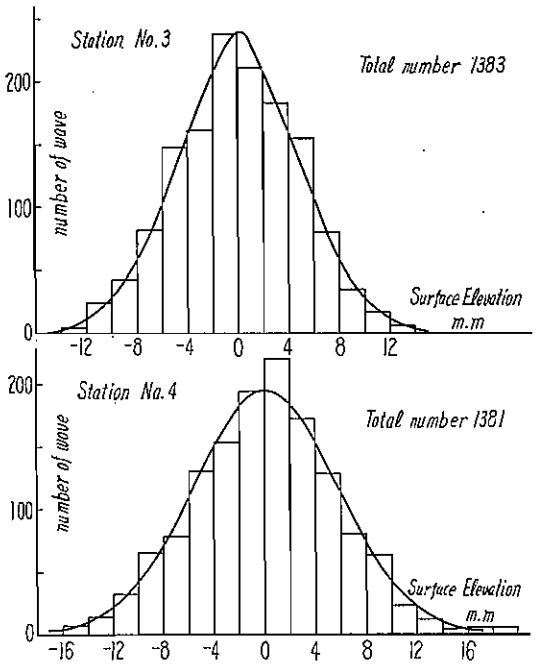

Fig 6-b. Histogram of Surface Elevation (r.p.m 300)

* Analysis of wave record at this time was done by using one-third of each wave record of 6 minutes, i. e., wave record of 2 minutes length from the beginning. Because such an analysis of wave record was very laborious and we had found in some particular case that the mean wave properties of 2 minute length had been not so different from that of 6 minute length record.

** In Fig-6~Fig-7, and in Table-5, the direct reading of the trace $y_{(t)}$ on the chart record was used instead of actual elevation of water surface $\eta_{(t)}$. That is, the calibration factors were not maltiplied to the values.

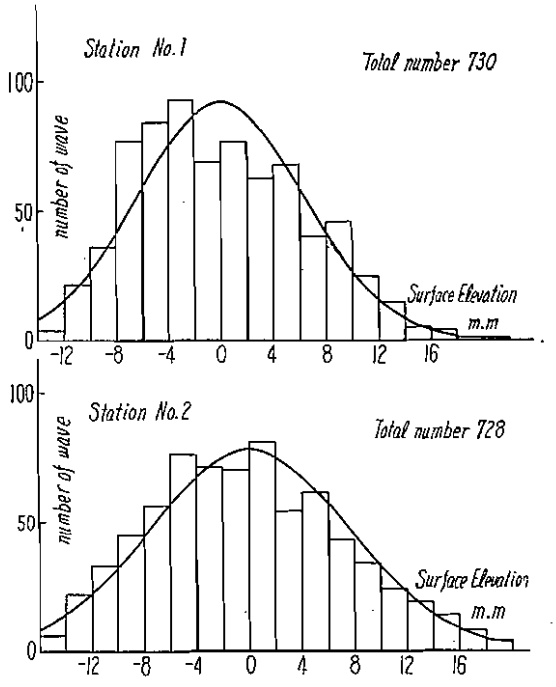

Fig 7-a. Histogram of Surface Elevation (r.p.m 400)

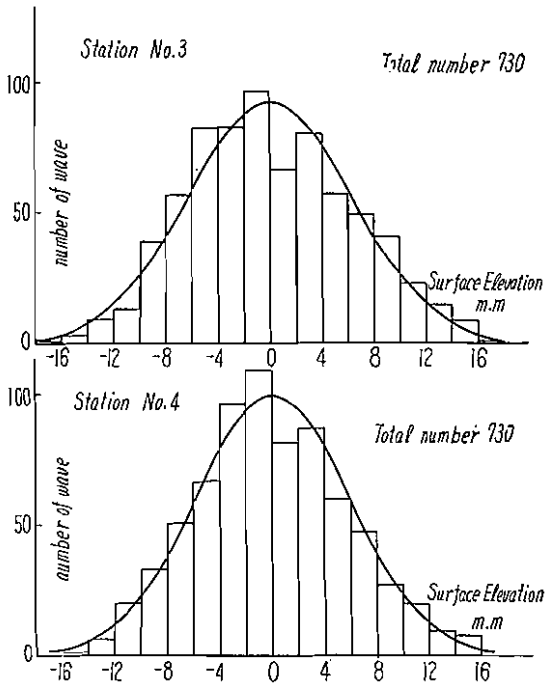

Fig 7-b. Histogram of Surface Elevation (r.p.m 400)

Table 5. Moments, Skewness, Kurtosis and Chi-Square

r.p.m.	Station	No. of wave	$\mu_2(=\overline{y^2})$	$\mu_3(=\overline{y^3})$	$\mu_4(=\overline{y^4})$	$\sqrt{\beta_1}$	β_2	χ^2	$p(\chi^2)$
300	1	1157	30.5	38.1	2.26	0.228	2.43	37.9	$\sim<0.01$
	2	1262	30.3	31.8	2.53	0.191	2.76	24.9	$\sim<0.01$
	3	1383	22.2	-5.40	1.43	-0.052	2.90	10.6	$0.3<\sim<0.5$
	4	1386	32.3	23.7	3.36	0.129	3.22	12.4	$0.2<\sim<0.3$
400	1	730	39.8	99.5	4.21	0.396	2.66	46.7	$\sim<0.01$
	2	728	55.7	138	8.79	0.332	2.83	13.7	$0.1<\sim<0.2$
	3	730	38.7	58.3	3.93	0.242	2.62	22.6	$\sim<0.01$
	4	730	33.7	36.2	3.05	0.185	2.69	7.50	$0.5<\sim<0.7$

our experimental cases. However, our data show that as the propagation of the wind waves in the calm area the deviation decreases gradually, i.e., the frequency distribution approaches approximately to the Gaussian, though the coincidence is still not so good. This may actually correspond the decrease of nonlinearity in wave form as can be seen in Figure 5 and described in section 3-1. In view of these results it can be said that in the wind wave of large wave

steepness the Gaussian process is not so good approximation and the deviation will mainly due to the nonlinearity of the wind wave as discussed by Longuet-Higgins (1963). However, in the wind wave of small steepness and especially in the waves in decay area where the high frequency ripples and also the nonlinearities are greatly diminished, the assumption of the Gaussian process will be good approximation.

3-3 Changes of Mean Wave Properties in Decay Area

In the decay area of our experimental flume there are no energy supply to wind waves from the outside. The energy of the waves should be only dissipated due to the bottom friction and side friction in the flume, air resistance, the internal friction and the interaction with the surface shear flow generated by the wind simultaneously with the wave.

There are few quantitative data about the damping of random waves, as far as we know. Our previous preliminary studies [Mitsuyasu(1958)] showed the interesting fact that slight increase of mean wave period occured associated with the decrease of wave height. This would suggest that period increase should be related to the change of wave spectrum. So the detailed analysis of the present wave record was conducted and finally compared with the properties of corresponding wave specrum.

The quantities calculated from the wave records were as follows:

(i) Wave period T defined as the time interval of successive zero-up-crossing and its mean value $\overline{T}$, standard deviation σ_T and confidence limit of the mean value.

(ii) Wave height H defined as the difference in water level between a crest (maximum) and the following trough (minimum), and its mean value $\overline{H}$, standard deviation σ_H and confidence limit of the mean value.

The wave properties at the various measuring points of decay area were summarized in Table 6a and Table 6b.

From these data it can be seen that the mean wave height $\overline{H}$ decrease gradally and mean wave period $\overline{T}$ increase slightly as the propagation of waves in the decaying area.*

As the wave heights and periods show much scattered values, the accuracy of the mean values in the statistical sense were examined formally by calculating

* In the case of r.p.m. 400 slight increase of wave height is seen at the Station No. 2 as compard the value of No. 1. This will perhaps be due to the special boundary condition at the trangent area from the generating area to decaying area as mentioned in section 3-1.

TABLE 6a

Wave Characteristics in Decay Area

(r.p.m.300)

Station	No. 1	No. 2	No. 3	No. 4
$\overline{T}$ sec	0.403	0.438	0.465	0.471
σ_T sec	0.090	0.089	0.079	0.090
N_T	298	274	258	254
$\frac{\sigma_T}{\sqrt{N_T}}t$ sec	±0.010	±0.011	±0.010	±0.011
$\overline{H}$ cm	2.05	1.41	1.28	1.12
σ_H cm	0.75	0.78	0.66	0.61
N_H	303	283	274	324
$\frac{\sigma_H}{\sqrt{N_H}}t$ cm	±0.11	±0.09	±0.07	±0.07
$\overline{\eta^2}$ cm	0.64 ±0.05	0.41 ±0.03	0.28 ±0.02	0.23 ±0.02
$\sqrt{\overline{\eta^2}}$ cm	0.80	0.64	0.53	0.48
$\overline{H}/\overline{\tilde{L}}$	0.081	0.047	0.038	0.025

* $\overline{\tilde{L}}=\frac{g\overline{T}^2}{2\pi}$

TABLE 6b

Wave Characteristics in Decay Area

(r.p.m.. 400)

Station	No.1	No.2	No.3	No.4
$\overline{T}$ sec	0.42	0.525	0.561	0.556
σ_T sec	0.091	0.078	0.101	0.134
N_T	269	243	213	223
$\frac{\sigma_T}{N_T}t$ sec	±0.011	±0.010	±0.014	±0.018
$\overline{H}$ cm	2.70	3.02	2.65	2.10
σ_H cm	1.16	1.42	1.25	1.30
N_H	286	236	225	237
$\frac{\sigma_H}{N_H}t_{(95\%)}$	0.13	0.18	0.16	0.17
$\overline{\eta^2}$ cm^2	1.10 ±0.11	1.35 ±0.14	0.96 ±0.1.	0.85 ±0.09
$\sqrt{\overline{\eta^2}}$ cm	1.05	1.16	0.98	0.92
$\overline{H}/\overline{\tilde{L}}$*	0.089	0.070	0.053	0.044

* $\overline{\tilde{L}}=\frac{g\overline{T}^2}{2\pi}$

the 95% confidence limit based on the t-distribution.*** That is, the following equations were used respectively to obtain the 95% confidence limits;

$$(\overline{T})_{95\%}=\overline{T}\pm\frac{\sigma_T}{N_T-1}t$$

$$(\overline{H})_{95\%}=\overline{H}\pm\frac{\sigma_H}{N_H-1}t$$

where:

$(\overline{T})_{95\%}$ = 95% confidence limit of mean wave period $\overline{T}$
$(\overline{H})_{95\%}$ = 95% confidence limit of mean wave height $\overline{H}$
σ_T = standard deviation of wave pariod
σ_H = standard deviation of wave height
N_T = number of the sample of wave period
N_H = number of the sample of wave height
t = student t corresponding to the freedom N_T-1 or N_H-1

As shown in Table 6a and Table 6b, even if the confidence limits are considered, we can conclude the decrease of wave height and increase of wave period. Figure. 8 shows general trend of the change of wave height and of wave period.

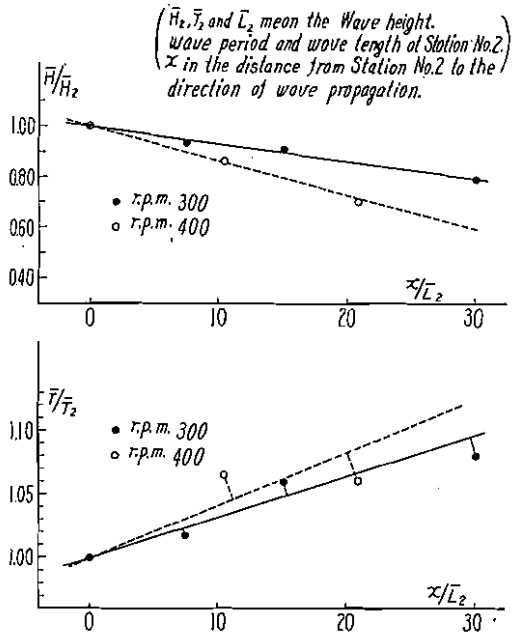

Fig.-8. Decrase of Wave Height and Increase of Wave Period in Decay Area

*** In the strict meaning, the application of the t-distribution would not be adequate because the frequency distributions of those values (wave period, wave height) were slightly different from the normal distributions. But, the deviation of those distributions from the normal distribution were not so conspicuous that the order of magnitude of confidence limit could be estimated from those values.

Moreover, it will be shown in the latter that such properties of waves in decaying area have close relation to their spectrum structures.

Table 7 shows the interrelations among the statistically defined mean wave

TABLE 7

Interrelation Among the Characteristic Mean Wave Height

r.p.m.	Station	No.1	No.2	No.3	No.4	Theory
300	$\overline{H}_{1/3}/\overline{H}$	1.45	1.51	1.59	1.61	1.59
	$\overline{H}_{1/10}/\overline{H}$	1.73	2.03	1.96	2.02	2.03
	$\overline{H}_{max}/\overline{H}$	2.04	2.70	2.28	2.62	2.70*
	$2\sqrt{\overline{\eta^2}}/\overline{H}$	0.78	0.71	0.83	0.86	0.798
400	$\overline{H}_{1/3}/\overline{H}$	1.47	1.48	1.50	1.65	1.59
	$\overline{H}_{1/10}/\overline{H}$	1.70	1.78	1.83	2.02	2.03
	$\overline{H}_{max}/\overline{H}$	2.20	2.16	2.37	2.62	2.70*
	$2\sqrt{\overline{\eta^2}}/\overline{H}$	0.78	0.77	0.74	0.88	0.798

* Theoretical maximum wave height was calculated as the most probable maximum height in 200 waves.

heights, i. e., mean wave height of total waves $\overline{H}$, mean wave height of highest one-third waves $\overline{H}_{1/3}$, mean wave height of highest 10% waves $\overline{H}_{1/10}$ and the highest wave H_{max} in each record. This table also includes the corresponding theoretical values derived by Longuet-Higgins (1952) under the assumptions of the narrow band spectrum and Gaussian process of the wind wave.

According to the present data on Table 7 the interrelations among these characteristic wave heights are not so well fit to the theoretical values in the generating area, but they approach gradually to the theoretical values as the propagtion of waves in decaying area. As shown in later paragraph the change of the band width of wave spectrum was not so conspicuous even in the decaying area of the flume. Therefore, the discrepncy between the theory and experimental results should be mainly due to the difference of actual wave property from the Gaussian model.

However, even in the generating area, discrepancies between the theoretical values and observed values are not so large. We will, therefore, be able to use the theoretical results for the practical purpose.

We also tried to compare the results with the theory of statistical properties of wave derived by Cartwright (1956) in which there is no restriction of narrow band spectrum. But we didn't proceed it due to some difficulties. In his

theory, surface elevation $\eta_{(t)}$ was assumed to be symmetrical about the mean water level (M.W.L) in the statistical sense and this is a consequence of Gaussian hypothesis. However, it was not correct in our actual wave data and η_+ (upward deviation of wate surface from M.W.L.) and the η_- (downward deviation of the water surface from M.W.L.) had slightly different statitical properties.

This could be expected when we remember the untisymmetrical wave form, i.e., sharp crest and flat trough in the steep wave, which is essentially due to non-linearity of wave.

The statistical distribution of $\eta(t)$ was compared with the Gram-Charlier series of the form used by Kinsman (1960). The agreements between the theory and experiment were slightly improved for the most part. But, in the case of generating area, the probabilities were still smaller than one percent for both cases, r.p.m. 300 and r.p.m. 400. This might reflect the strong nonlinearity of the wind wave in the generating area of our wave tank. The statistical distribution of the Gram-Charlier type has been derived on the assumption of "weakly non-linear".

§4. Specbrum of Wind Woves in Decry Area

4-1. Wave spectrum (defintion and its general properties)

The magnetic tape which contained the six minutes record of wind wave was spliced into three pieces of equal length and made to loops. Such looped tapes of two minutes length were analyzed successively and their Fourier spectrum were recorded on chart papers. The spectrum record on the chart paper was measured and read out at the interval of 0.05 C/S in the original frequency scale (not in the 40 times increased frequency scale).

After taking the mean values of corresponding three records measured values were squared and multiplied by the calibration factor to obtain the power spectrum. The spectrum density $\phi_{(f)}$ was finally obtained by dividing the above obtained values with the effective band width of the filter. The spectrum density which we obtained satisfied the following relation principally

$$\int_0^\infty \phi_{(f)} df = \overline{\eta^2} \qquad (3)$$

Figure 9a and Figure 9b show one-dimensional frequency spectra of wind waves which obtained respectively in each measuring station on the decay area.

One of the remarkable characteristics of the spectrum in decay area is the downward shift of the frequency f_{max} at which the spectrum density is maximum, much amount of energy dissipation near the dominant peak of wave spectrum and the trend of energy transfer from high frequency range to the low frequency

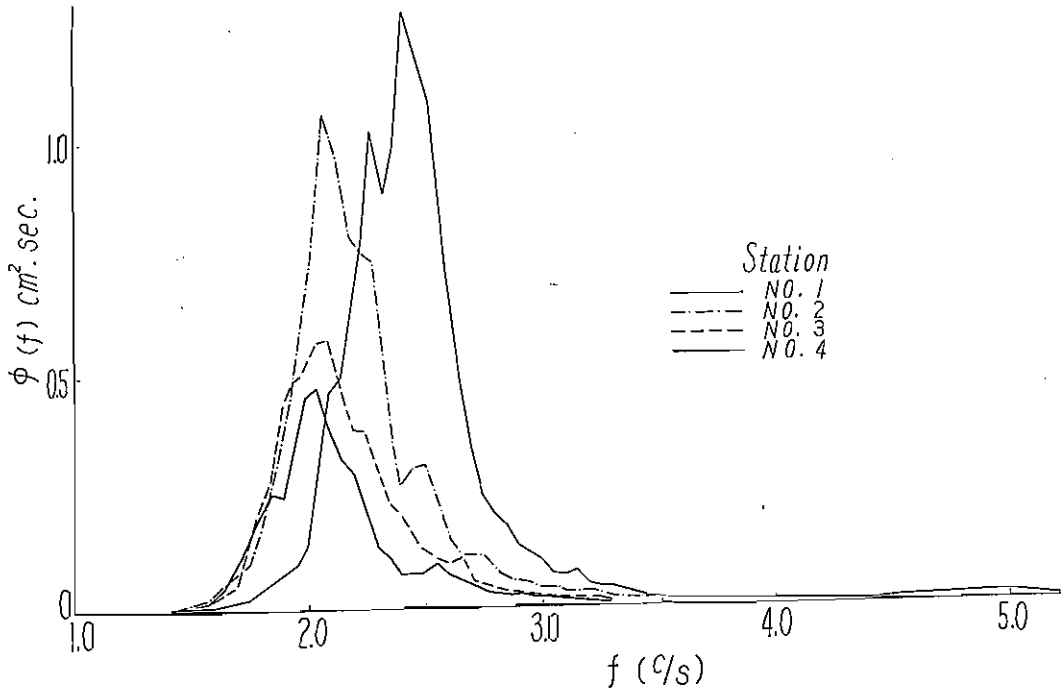

Fig-9a. Spectrum of Wind Wave (r.p.m 300)

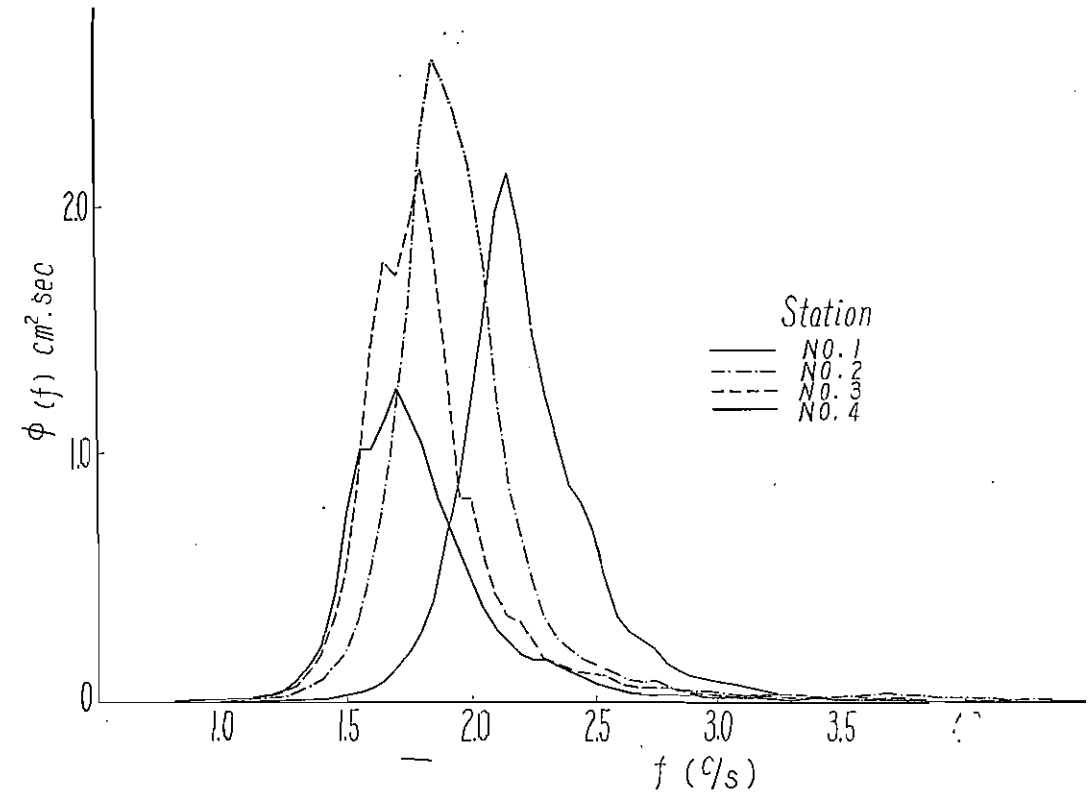

Fig-9b. Spectrum of Wind Wave (r.p.m 400)

range which occurred conspicuously between the station No. 1 and No. 2.

The area between the Station No. 1 and No. 2 is, as it were, transition area. So their special boundary condition will affect the wave in a complicated way. However, this phenomena may not necessary be attributed only to the special boundary conditions, because in the case of r.p.m. 400 similer trend can be found even in the area between the Station No. 2 and No. 3 where the wind is not blowing and there are no change of boundary conditions throughout this area. As we had paid much care to the accuracy of frequency of spectrum, this could not be attributed to the error of measurement.

The only thing which can be said at this stage based on the experimental evidence is that this energy transfer from high frequency to low frequency seems to have a closed relation to the large scale breaking of the waves.

As described in 3-1, at the area between the station No. 1 and No. 2 waves were breaking in large scale and gradually becoming smooth. In the case of r.p.m. 400, breaking of waves occurred even at the area between the station No.2 and No. 3. On the other hand, at the area between Station No. 2 and No. 4 in the case of r.p.m. 300 and between Station No.3 and No. 4 in the case of r.p.m. 400, where the waves were relatively smooth and not breaking, no such energy transfers were observed.

As far as we know, there are no theoretical works which explained such a mechanism of energy transfer.* However, above facts suggest that in the generating area a part of the wave energy is transfered from high frequency part to the low frequency part through the special mechanism and that this special mechanism seems to have a closed relation to the breaking of waves.

According to the hitherto considerations a part of wave energy is lost by breaking and this energy flows into turbulence or short ripples and finally to the heat through drift current. Our present results suggest the other way of energy flow through breaking of waves.

Apart from such a mechanism of energy transfer above mentioned, the frequency f_{max} at the maximum of spectral density $[\phi(f)]_{max}$ was compared with the mean wave period $\overline{T}$ obtained from the wave record. At the same time average wave period was computed by using measured wave spectrum through the following equation

---

* About ten years ago Yoshida (1951) considered the energy transfer from high frequency to low frequency through breaking to explain the growth of wind waves. According to his descriptions "the breaking of each component wave may occur with almost irregular intervals, but occurs with larger interval than each own period and especially seems to do most frequently with period and especially seems to do most frequently with period of significant wave".

$$\bar{\bar{T}}=\left[\frac{\int_0^\infty \phi_{(f)}df}{\int_0^\infty f^2\phi_{(f)}df}\right]^{\frac{1}{2}} \qquad (4)$$

Obtained results are summarized in Table 8 with the other characteristic

Table 8 Wave Period, Wave Energy and Spectrum Width

Station / r.p.m.		No. 1	No. 2	No. 3	No. 4
300	$T_1(=1/\text{fmax})$	0.408	0.476	0.483	0.495
	$T_1/\overline{T}$	1.01	1.09	1.04	1.05
	$\bar{\bar{T}}$	0.392	0.436	0.418	0.457
	$\bar{\bar{T}}/\overline{T}$	0.973	0.995	0.899	0.970
	$\int_0^\infty \phi_{(f)}df$	0.643	0.500	0.316	0.224
	$\overline{\eta^2}/\int_0^\infty \phi_{(f)}df$	0.995	0.803	0.874	1.009
	ε	0.46	0.43	0.35	0.35
400	$T_1(=1/\text{fmax})$	0.465	0.540	0.555	0.588
	$T_1/\overline{T}$	1.05	1.03	0.99	1.05
	$\bar{\bar{T}}$	0.499	0.496	0.522	0.538
	$\bar{\bar{T}}/\overline{T}$	1.13	0.946	0.933	0.965
	$\int_0^\infty \phi_{(f)}df$	1.038	1.228	1.000	0.678
	$\overline{\eta^2}/\int_0^\infty \phi_{(f)}df$	1.06	1.10	0.96	1.25
	ε	0.52	0.46	0.53	0.44

quantities of wave spectrum such as, total wave energy $\int_0^\infty \phi_{(f)}df$, thier ratio to the mean square elevation of water surface $\overline{\eta^2}$, and spectrum widte ε defined by Cartwright (1956).

$$\varepsilon^2=\frac{m_0m_4-m_2^2}{m_0m_4} \qquad (5)$$

where
$$m_n=\int_0^\infty \phi_{(f)}f^n df \qquad (6)$$

According to the results shown in Table 8, characteristic wave periods obtained by the different methods agree quite well in each other as predicted by J. W. Pierson (1954). Moreover, every wave period obtained by different way show the increase as the propagation of the waves in decay area.

From these results we can see that the increase of mean wave period is closely related to the deformation of wave spectrum, although the mechanism of the deformation of the spectrum are still not clear.* Some of them can be attributed to the energy loss due to viscosity of water and to air resistance, some of them to nonlinear interaction and some of them to breaking of waves and ripple formation. However, as shown later, energy loss due to moleculer viscosity seems to fail to explain the energy loss near the peak of energy spectrum. And also the theory of non-linear interaction seems to be difficult to give an adequate solution at this stage, because the time scale of the actual phenomena is too short as compared the characteristic time scale of the energy flux estimated by theory. That is, according to Hasselman (1961) characteristic time Tc of energy flux was given by $Tc \sim \overline{T}\, S^{-4}$. Here $\overline{T}$ is a suitably defined mean wave period and S is the root mean square wave slope. Assuming the proportionality factor equal to one and also $S \fallingdotseq 1/5$ as referred to Cox's (1958) data, we can find that for $\overline{T} \fallingdotseq 0.5$ in our experimental case $Tc \fallingdotseq 313$ sec.

On the other hand, the elapsed time of wave propagation from one measuring station to the next station in our experimental condition is the order of

$$t = d/\bar{c} = 450\ \text{cm}/80\ \text{cm/sec} = 5.63\ \text{sec}.$$

Here d is the distance between two successive measuring stations and $\bar{c}$ is the suitably defined mean wave velocity.

This difference in the time scale is too large to explain the actual present phenomena with the theory of non-linear interaction.

4-2 Decay of the energy of wave spectrum

As shown in Table 8, total energy of wave spectrum obtained by the numerical integration of measured spectrum were very close to the mean-square surface elevation $\overline{\eta^2}$ at every location in the decay area, and total energy decreased as the propagation of waves. The energy loss in the wind wave must be due to the viscous energy dissipation in the boundary layer near the side wall and in the surface shear zone, the energy transfer from the wave mode to the turblent vortex mode which is caused by breaking of wave or by the non-linear interaction with the other mode of motion, the energy transfer to air and the energy dissipation by overlapping ripples. Bottom friction should be negligible in our case because the wave lengths are relatively small.

As the theoretical consideration of the experimental results including all of

* In our experimental condition, the segregation of the component wave due to the difference of wave velocity would not occur. Because, the system of motion is stationary, i.e., the wind waves were stationaly propagating from the generating area to the decay area in respect of time.

these effects are extremely difficult, we will not discuss this problem at this time in detail, and only show the comparison of the experimental results with the results obtained by only considering the viscous energy dissiptions in the boundary layer near the side wall and in the surface shear zone. Moreover, it will be checked how this treatment can explain the actual phenomena or how the actual situations are different from what was predicted by this treatment.

By only considering the energy dissipation due to moleculer viscosity the decay of wave energy can be given (c.f. appendix)

$$E_{(f,x)}=E_{0(f)}\cdot\exp-\left(\frac{256\pi^5\nu}{g^3}f^5+\frac{8\pi}{bg}\sqrt{\pi\nu}f^{3/2}\right)x \qquad (7)$$

where $E_{(f,x)}$=total energy of waves as the function of frequency and position x,

ν=kinetic viscosity (0.016)

g=acceleration of gravity (980 dyn)

b=width of the wave tank (150 cm)

If we neglect the non-linear interaction among the component waves the decay of energy of wave spectrum due to molecular viscosity can be obtained by replacing $E_{(f,x)}$ with the spectrum of wave $\phi_{(f,x)}$

$$\phi_{(f,x)}=\phi_{0(f)}\exp-\left(\frac{256\pi\nu x}{g^3}f^5+\frac{8\pi x}{bg}\sqrt{\pi\nu}f^{3/2}\right) \qquad (8)$$

Calculated spectrum $\phi_{(f,x)}$ were compared with the measured spectrum and shown in Figure 10a~Figure 10d in the logarithmic scale.

According to those results fairly good agreement found only at high frequency range, and many discrepancies happened near the frequenc at the peak of the energy density. These discrepyncies may be due to the other mechanisms neglected in the equation of decay of energy spectrum.

To see this peculiar property more in detailes, we introduce the rate of the

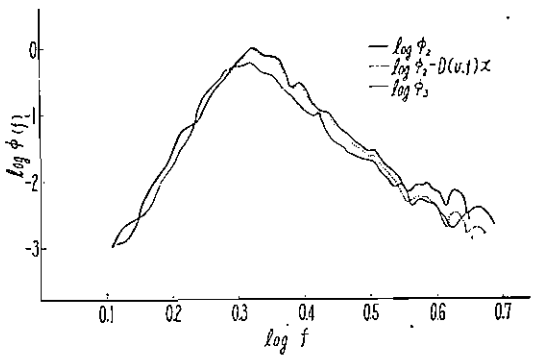

Fig10-a. Spectrum of Wind Wave (r.p.m 300, station 2~3)

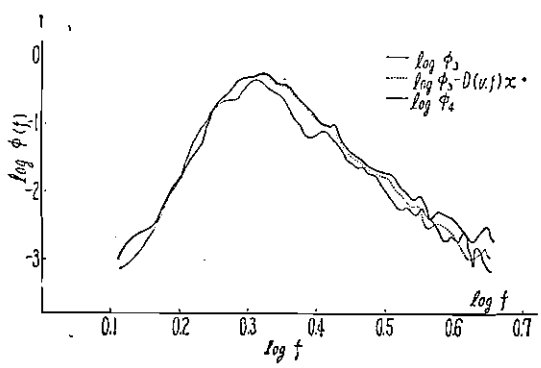

Fig10-b Spectrum of Wind Wave (r.p.m 300, station 3~4)

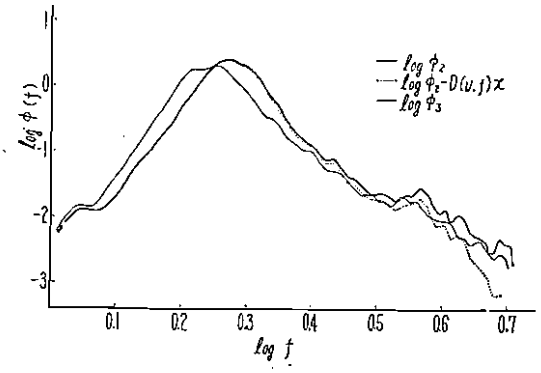

Fig10-c. Spectrum of Wind Wave (r.p.m 400, station 2~3)

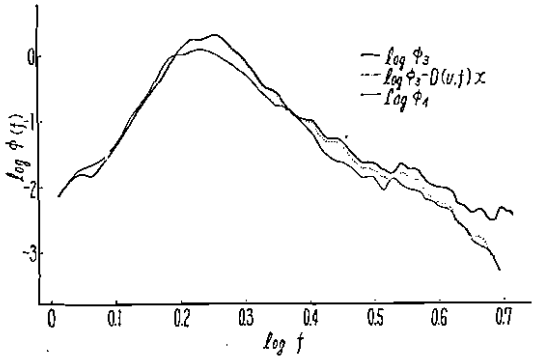

Fig10-d Spectrum of Wind Wave (r.p.m 400, station 3~4)

apparent energy transfer $T_{*(f,x)}$ analogous to the equation governing the spectrum of turbulence.* Then the equation for the wave spectrum is

$$\frac{\partial \phi_{(f,x)}}{\partial x} = T_{*(f,x)} - D_{(\nu,f)}\phi_{(f,x)} \tag{9}$$

where

$$D_{(\nu,f)} = \left(\frac{256\pi^5\nu}{g^3}f^5 + \frac{8\pi}{bg}\sqrt{\pi\nu}f^{3/2}\right) \tag{10}$$

or by introducing the transfer function

$$S_{(f,x)} = -\int_0^f T_{*(f',x)}df' \tag{11}$$

we can obtain

$$\frac{\partial \phi}{\partial x} = -\frac{\partial S}{\partial f} - D\phi \tag{12}$$

If there are no any other loss except for what were included in the equation (10)

$$\int_0^\infty \frac{\partial \phi}{\partial x}df = -\int_0^\infty D_{(\nu,f)}\phi_{(f,x)}df \tag{13}$$

since the total transfer due to the wave motion is zero,

$$\int_0^\infty T_{*(f,x)}df = 0 \tag{14}$$

The rate of energy transfer T_* and the energy transfer function S determined respectively from Eq. (9) and Eq. (11) using measured rates of change of spectrum

* At this time, the introduction of T_* is only a matter of convenience, because the physical meaning of T_* is obscure as compared the rate of energy transfer in the turbulence. In addition to the actual energy transfer among the components of waves, T_* may include the energy dissipation neglected in $D(\nu,f)$ and the energy transfer from wave motion to the other mode of motion like turbulence.

and energy dissipation are shown in Fig. 11 and Fig. 12.

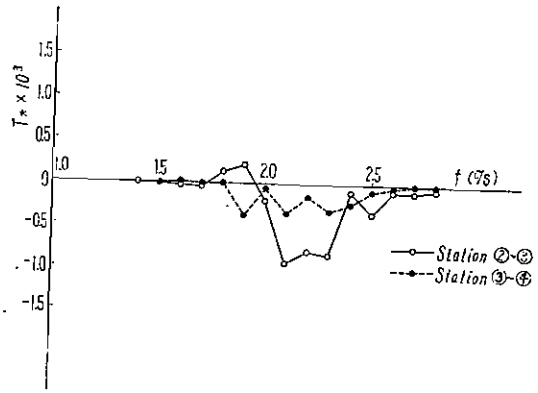

Fig11-a Energy Transfer Rate
(r.p.m 300)

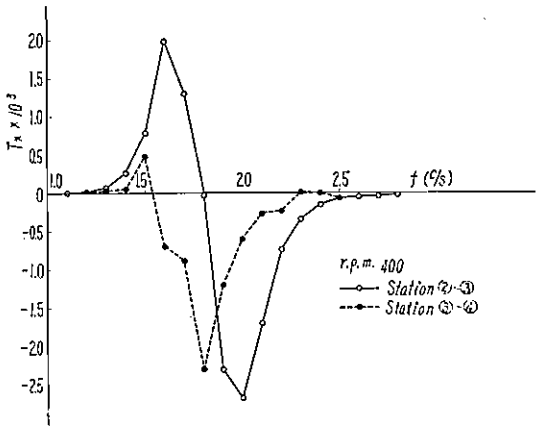

Fig-11b. Energy Transfer Rate
(r.p.m 400)

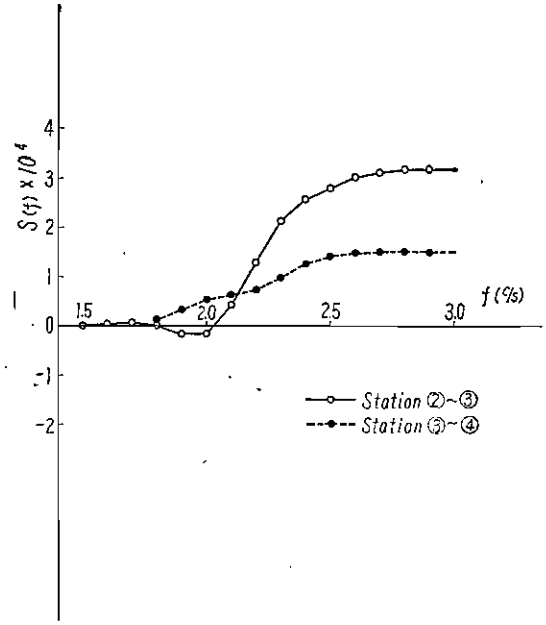

Fig12-a Transfer Function
(r.p.m 300)

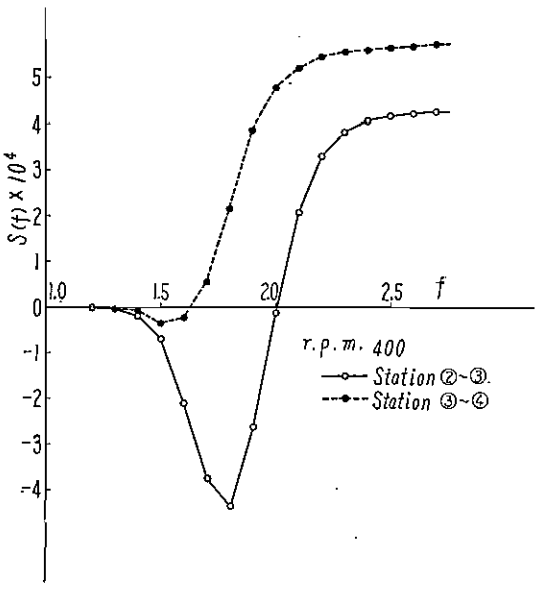

Fig12-b Transfer Function
(r.p.m 400)

As was expected from Fig. 10, Fig. 11 shows clearly the energy accumulation in some low frequency range and energy loss in some high frequency range. If this is due to the energy transfer by non-linear interaction of waves and there is no any other energy dissipation except for what was considered in Eq. 9 and Eq. 10, then integration of T_{*} with respect to f, from zero to infinity, must be zero. But

* In those computations confidence bands were not considered. Therefore, those absolute values include the uncertainties in the statistical sense. However, it was found that such a energy transfer could'nt be neglected even when the confidence bond was considered.

this is not satisfactory as shown in Fig. 12. According to Fig. 12b, the energy is transferred from high frequency to low frequency at the frequency range lower than f_2 and the energy transfer is maximum at frequency f_1, and zero at the frequency f_2 (c.f. Fig 13).

However, even above the frequency f_2, there is a large amount of apparent energy transfer of the opposite direction. If we consider this energy transfer is the actual transfer, above result shows that the energy in the wave spectrum is transferred from low frequency to high frequency at the frequency range greater than f_2, and above the frequency f_3 this energy transfer is constant i. e., energy is transferred without accumulation or dissipation. But this model will not be reasonable because this is contradictory to the energy conservation law without introducing additional artificial energy dissipation.

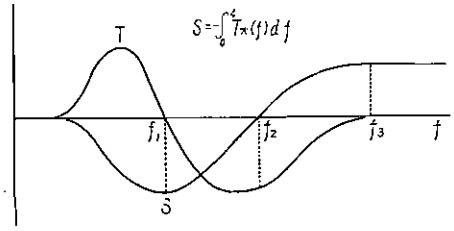

Fig. 13. Schematic Representation of the Rate of Energy Transfer $T_{ii}(f)$ and Transfer Function S(f)

On the other hand, we can interpret these results as the selective energy dissipation due to the breaking of wave, interaction with the turbulent surface shear flow and formation of overlapping ripples. Fig. 12a, which shows the results obtained in non-breaking region indicates much different characteristics. That is, there are no such frequency range of energy transfer from high to low as in the case shown in Fig. 12b and there exists only the frequency range of additional energy dissipation.

From these results it can be conjectured about the decay of wave spectrum that (i) the energy at the high frequency range, approximately greater than f_3= 3 c/s in our cace, is dissipated by molecular viscosity, (ii) the energy in the frequency range between f_1 and f_3 is transferred partly to the low frequency range of the wave spectrum and partly to the turbulence through breaking of waves and the other unknown mechamisum* and (iii) the remaining parts of the energy in that frequency range are selectively dissipated by the interaction with the air and the formation of overlapping ripples. At present now, however, we have few knowledge about the quantitative participations of those mechanisums of energy dissipation in the wave spectrum.

It is also very interesting that, as will be shown in next section, this region

* Recently, Hamada (1964) has proposed theoretically the mechanisum to generate the turbulent vortex from the wave motion if the slope of the wave spectrum is steeper than "−5 power".

in the spectrum has an excess energy as compared to the equilibrium form of spectrum.

4-3 Similarity of the spectrum of wind wave

Great many studies have been done on the form of spectrum of wind waves. Some of them are based on field observation and used for the practical forecasting of waves and some of them are based on theoretical considerations and discussed to clarify the physical mechanism of the motion of wind waves.

With reference to the high frequency part, Phillips (1958), from a consideration of limiting configuration of surface wave, showed that an equilibrium range may exist, and by dimensional argument he derived a "-5 power law"for it.

Pierson (1959) discussed the frequency range where the equilibrium range could be expected and showed, based on the nonlinear theory developed by Tick (1959), that the equilibrium range should exist in some frequency range greater than twice of the frequency of major power peak in the spectrum. Kinsman (1961) also discussed this problem by using his results of observation.

Recently, Kitaigorodski (1962) extensively applied the similarity theory to the description of wave spectra. By the close analogy with the spectrum of turbulence, he divided the wave spectrum to various frequency ranges which respectively have different main controlling factors as schematically shown in Fig. 14.

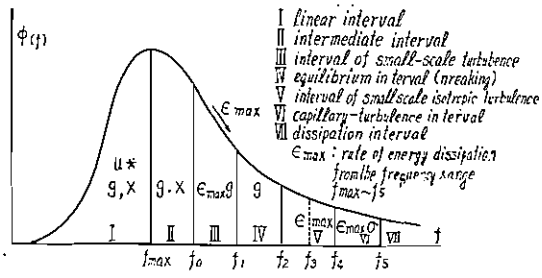

Fig. 14· Schematic Representation of the Narrow Spectrum of Wind Wave

He conjectured that the wave spectrum near the frequency of maximum energy density could be expressed as

$$\phi(\omega)=g^2\omega^{-5}F_1\left(\frac{u_{*}\omega}{g},\ \frac{gX}{u^{*2}}\right) \tag{15}$$

where

ω = angular frequency

u_{*} = friction velocity of the wind

X = fetch

He also determined, based on Burling's results and his own results, the actual form of the spectrum in the frequency range smaller than dominant peak and showed

$$\log \frac{\phi(\omega)\omega^5}{g^2} = a + b\frac{u^{*}\omega}{g} \tag{16}$$

where

a and b are dimensionless coefficients and may only depend on the dimensionless fetch. He obtained $a=-8.59\sim-9.62$, $b=31\sim46$ by using Burling's (1959) data.

Fig. 15a and Fig. 15b show our experimental results expressed in the same universal form as Kitaigorodski's one. In our decay area, there never exists a

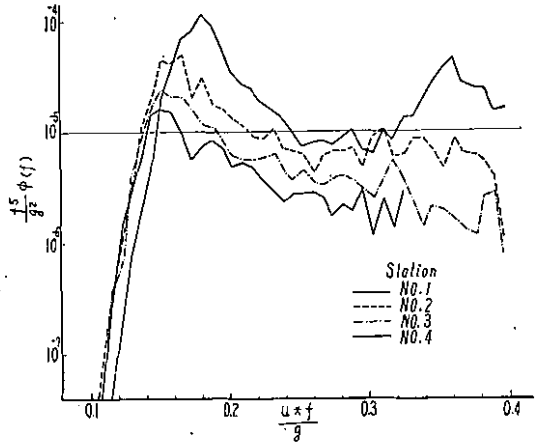

Fig15-a. Spectrum of Wind Wave (r.p.m 300) normalized by Eq. (15)

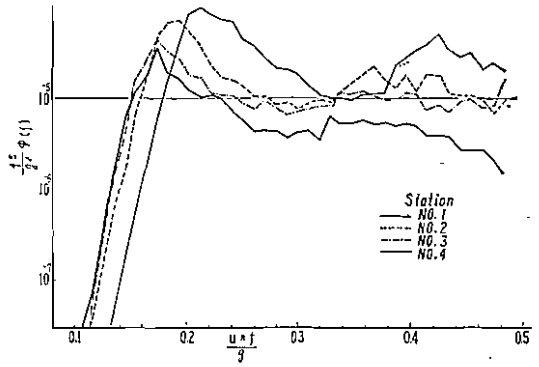

Fig-15-b. Spectrum of Wind Wave(r.p.m 400) normalized by Eq. (15)

wind, and therefore, u_{*} were actually zero. However, approximate values of u_{*} near the end of generating area were used for the convenience of the comparison of our data with the other data.

In spite of our very short limited fetch wave spectrum agrees fairly well with the universal form proposed by Kitaigorodski as the general trend. However, there can be seen several conspicuous characteristics of our measured spectrum, i.e., (i) excess energy near the dominant peak of energy density and (ii) secondary peak of the energy density near the twice of the frequency of dominant peak.

This secondary peak may correspond exactly to the nonlinear effect suggested by Tick (1959) and Pierson (1959) and, in this respect, the equilibrium range does not exist in our spectrum in the strict sense suggested by Pierson, or even if it exists we cannot see them because of their extremely low energy densty.
As the propagation of the waves in decay area, as will be expected, this secondary peak gradually decreased reflecting the decrease of non-linearlty of the waves,

and the spectrum approached very close to the universal form. And after that the high frequency part of the spectrum decayed gradually due to the molecular viscosity as discussed in the previous section.

In the case of r.p.m. 300 wave spectrum seemed not to attain the saturated condition, because the energy density at the high frequency range were slightly lower than the universal form.

As the maximum frequency of our measured spectrum, which had detectable energy density was approximately 5 c/s, the effect of the surface tension would be not so important in all frequency range of our measured spectrum.

The excess energy near the frequency of the maximum energy density, dominant peak of the spectrum, was very peculiar phenomenon.

The similar trend of excess energy concentration near the dominant peak in the spectrum could be seen in the slope spectrum measured by Cox (1958) in his wave tank of small scale. On the other hand, in Burling's (1959) spectrum, or in the SWOP data quoted by Phillips (1961), that were obtained in the field, such a trend couldn't be seen.

Therefore, excess energy concentration in our measured spectrum might be attributed to the short fetch or special conditions in the wind flume, i.e. limited width of tank, wind velocity distribution, pressure distribution, or regularity of wind direction and steadiness of wind speed, etc. Some explanation will be given by the short fetch of wind flume. Due to the short fetch wind wave of strongly non-linear has no sufficient time to exchange energy among the frequencies through non-linear interaction and become weakly non-linear. In this respect, this energy conentration means the strong nonlinearity of the waves generated in the wind flume. It is very intersesting, at this time, to remember that we observed the energy transfer from this range to lower frequency range and also the energy dissipations much greater than what we expected based on the effect of molecular viscosity.

As suggested by Kitaigorodski (1962), the spectrum in the frequency range lower than the dominant peak of the spectrum could well be distinguished by

$$\log \frac{\phi(f) f^5}{g^2} = A + B\frac{u^* f}{g} \tag{17}$$

although our dimensionless coefficients A and B were slightly different from Kitaigorodski's values. Cofficients A and B were determined by using the data in Fig 15a and Fig 15b and then those coefficients were converted to a and b in Kitaigorodski's expression Eq. (16). The constant a and b such determined are listed in Table 9. Apart from the slight difference of the values between r.p.m. 300 and r.p.m. 400, the obtained values of a and b are smaller than corresponding

Table

Values of Coefficient a and b in the formula (16)

r.p.m.	Station	a	b
300	1	−13	11
	2	−13	12
	3	−13	13
	4	−14	14
	(mean)	(−13)	(13)
400	1	−12	8.6
	2	−10	8.7
	3	−11	9.6
	4	−11	9.4
	(mean)	(−11)	(9.1)

Kitaigorodski's values. This means that our spectrum is shifted to higher frequency range than Burling's spectrum and that the slope of our spectrum in the frequency range lower than dominant peaks is smaller than Burling's one. This difference in the form of spectrum should be attributed to the difference of fetch, because the spectrum near the frequency of dominant peak and the spectrum in the frequency range lower than dominant peak strongly depend on the fetch.

Acknowledgement

The experimental work of this study was conducted in Hydraulic Laboratory of Port and Harbour Technical Research Institute during 1962. The authors are indebted to Dr. T. Hamada for his encouragement in the course of this work. Thanks are also due to Mrs. Kinoe, Miss. Ogasahara and Miss Nakajo of the Hydraulic Laboratory for their assistance in the data analysis and various numerical calculations.

A first draft of this paper was writen in 1963 when one of the author had been in the Department of Oceanography. of Texas A & M University. The authors wish to express their gratitude to Professor R. O. Reid for valuable comments on the first draft. Thanks are also due to Mr. L. Brennan and Mr. C. Bedoya who made the numerical calculation of rate of transfer and transfer function and to Mrs. J. Shaver who did the typing of first draft of this paper.

APPENDIX

Decay of Wave Energy in Wave Tank

The energy budget of wave in the tank can be given:

$$\frac{\partial E}{\partial t}=R-\frac{\partial}{\partial x}(C_gE) \tag{A-1}$$

where $E=$ wave energy per unit area
$R=$ rate of energy transfer to and from the mode of wave motion
$Cg=$ group velocity of wave.

In the steady condition

$$\frac{\partial E}{\partial t}=0 \tag{A-2}$$

In the case of deep water wave $Cg=\frac{1}{2}$c (c: phase velocity) and c is independent of x

$$\frac{\partial}{\partial x}(C_gE)=\frac{1}{2}E\frac{\partial c}{\partial x}+\frac{c}{2}\frac{\partial E}{\partial x}=\frac{c}{2}\frac{\partial E}{\partial x} \tag{A-3}$$

R should include:

(1) Viscous energy dissipation in the boundary layer near side walls and bottom ($(R\mu)si$, $(R\mu)b$),

(2) Viscous energy dissipation in the surface shear zone ($(R\mu)su$),

(3) Energydissipation due to radiation stress by ripple which is generated by surface tension and overlapps on the dominant wave (Rr),

(4) Transfer of energy from gravity wave mode to turbulent vortex modes (Rt). This will be due to non-linear interaction with the other modes of motion or due to breaking.

(5) Energy transfer to or from the air (Ra).

$(R\mu)$ b is neglisible in our present case due to relatively short wave length and $(R\mu)$ si per unit width and length can be given (Keulegan 1950)

$$(R\mu)si=-\frac{1}{b}\rho_w a^2c^2k\sqrt{\frac{kc\nu}{2}} \tag{A-4}$$

where $b=$ width of wave tank (150cm)
$\rho_w=$ density of water (1.00)
$a=$ amplitude of wave ($=H/2$)
$k=$ wave number ($=2\pi/L$)
$\nu=$ kinetic viscosity of water (0.0106)

$(R\mu)su$ per unit surface can be given (Lamb 1932)

$$(R\mu)su=-2\rho_w\nu a^2c^2k^3 \tag{A-5}$$

As the quantitative estimations of (3) Rr and (4) Rt are very difficult at present stage those terms will not be included in our present calculations.

There are no energy transfers from air to water in our experimental condition, and the energy loss due to air rcsistance (normat stress) may be approximated (Sverdrup and Munk 1957)

$$R_N=-\frac{1}{2}s\rho_a a^2c^3k^2 \tag{A-6}$$

where s=sheltering coefficient

ρ_a=density of air (0.0012).

However, this term will not be considered in the present calculation from the following reason;

(i) there exist at present much obscurity about the value of sheltering coefficient, and its physical meaning is not clear, and (ii) the effect of the air resistance seems not to be so critical* in the energy loss of wind wave in our experimental condition.

Finally, due to the situations discussed now, only the energy dissipations in the boundary layer near the side wall and in the surface shear zone will be considered in R. Then, substituting (A-2), (A-3), (A-4) and (A-5) to (A-1), *Eq.* (A-1) can be written in the form

$$\begin{aligned}\frac{c}{2}\frac{\partial E}{\partial x}=R&=-2\rho_w\nu a^2c^2k^3-\frac{1}{b}\rho_\omega a^2c^2k\sqrt{\frac{kc\nu}{2}}\\&=-\left(\frac{1}{2}\rho_\omega a^2c^2k\right)\left\{4\nu k^2+\frac{2}{b}\sqrt{\frac{kc\nu}{2}}\,.\right\}\\\frac{c}{2}\frac{\partial E}{\partial x}&=-E\left\{4\nu k^2+\frac{2}{b}\sqrt{\frac{kc\nu}{2}}\right\}\end{aligned} \tag{A-7}$$

The solution of this equation is

$$E=E_0\exp-\left\{\frac{8\nu k^2}{c}+\frac{2}{b}\sqrt{\frac{2k\nu}{c}}\right\}x \tag{A-8}$$

---

* If we consider the magnitude of each energy loss relative to the energy loss in the surface shear zone we can get from (A-4), (A-5) and (A-6)

$$(R_\mu)si/(R_\mu)su=36.5/f^{7/2}$$
$$R_N/(R_\mu)su=4.37/f^3$$

In the calculation of second relation sheltering coefficient was assument to be 0.04. Those relations indicate that the energy dissipation at the side walls is dominant in the low frequency range, and the energy dissipation at the surface shear zone is important in the high frequency range. In the frequency range lower than $f=1.6\,c/s$ the energy loss due to air resistance is larger than that in surface shear zone, but energy loss at the side wall is much larger than that in surface shear zone even in this frequency range.

In the case of actual ocean, the situation will be slightly different from our present estimations. Because there are no side walls and the wave frequency is much lower than that in our present experiment.

where E_0 is the wave energy at $x=0$

Since

$$c=g/2\pi f \tag{A-9}$$

and

$$k=(2\pi)^2 f^2/g \tag{A-10}$$

Eq. A-8 can be writen in the form

$$E=E_0\exp-\left\{\frac{256\pi^5\nu}{g^3}f^5+\frac{2}{b}\sqrt{\frac{16\pi^3 f^3\nu}{g^2}}\right\}x$$

$$=E_0\exp-\left\{\frac{256\pi^5\nu}{g^3}f^5+\frac{8\pi}{bg}\sqrt{\pi\nu}f^{2/3}\right\}x \tag{A-11}$$

References

Barber, N. A. and A. Ursell. 1948. The generation and propagation of ocean wave and swell. Trans. Roy. Soc. (London). Vol. 240, No. 824, 527-560.

Burling, R. W. 1959. The spectrum of waves on short fetches. Deutchen Hydrogr. Zeit. Vol. 12, 2-3.

Chang, S 1954. A magnetic tape wave recorder and energy spectrum analyzer for the analysis of ocean wave records. Beach Erosion Board Tech. Memo. No. 58.

Cartwright, D. E. and M. S. Longuet Higgins. 1956. The statistical distribution of the maxima of random function. Proc. Roy. Soc. A. Vol. 237, 212-232.

Cox, C. S. 1958. Measurement of slopes of high-frequency wind waves. J. Mar. Res. 16, 199-225.

Grone. P. and R. Drestein. 1950. Ocean swell; its decay and period increase. Nature. 165, 445.

Hasselman, K. 1961. On the non-linear energy transfer in a wave spectrum. Proc. Conference on Ocean Wave Spectra (Easton). 191-197.

Keulegan, G. H. 1950. The grodual damping of progressive oscillatory wave with distance in a prismatic rectangular channel. Report Bureau of Standards.

Kinsman, B. 1960. Surface waves at short fetches and low wind speeds. Chesapeake Bay Inst., Tech. Rep. 19.

——. 1961. Some evidence on the effect of non-linearity on the position of equilibrium range in wind-wave spectra. J. Geophys. Res. Vol. 66, No. 8, 2411-2415.

Kitaigorodski, S. A. 1962. Applications of the theory of similarity to the analysis of wind-generated wave motion as a stochastic process. Bull. I. Z. V. Geophys. Ser. No. 1, 73-80.

Lamb, Sir H. 1932. Hydrodynamics. 6th Ed.

Hamada T. 1964. On the "−5 power law" in wind wave spectrum. Abstracts of papers, the Conference of Japan Oceanographic Society in 1964, (unpublished)

Longuet-Higgins, M. S. 1952. On the statistical distribution of height of sea waves. J. Mar. Res., Vol. 11, No. 13, 245-266.

——. 1963. The generation of capillary waves by steep gravity waves. J.Fluid. Mech. Vol. 16, Part 1, 138-159.

——. 1963. The effect of non-linearities on statistical distributions in the theory of sea waves. J. Fluid Mech. vol 17, Part 3, 459-480.

Marks, W. and P. E. Strausser. 1960. SEADAC, The Taylor model basin seakeeping data analysis center, Report 1353.

Milles, J. W. 1962. On the generation of waves by shear flows. Part 4. J. Fluid Mech., 13, 433-448.

Mitsuyasu, H. and H. Haranaka. 1958. On the wind waves in decay area. Proc. Conference in Transportation Tech. Res. Inst. (Abstract).

Phillips, O. M. 1958. The equilibrium range in the spectrum of wind-generated waves. J. Mar. Res., Vol. 16, No. 3, 426-434.

——. 1961. The dynamics of random finite amplitude gravity waves. Proc. Conference Ocean Wave Spectra (Easton), 171-178.

Pierson, W. J. 1954. An electronic wave spectrum analyzer and its use in engineering problems. Beach Erosion Board Tech. Memo. No. 56.

——. 1959. A note on the growth of the spectrum of wind-generated gravity waves as determined by non-linear consideration. J. Geophys. Res., Vol. 64, No. 8, 1007-1011.

——. and W. Marks. 1952. The power spectrum analysis of ocean wave record. Trans. Amer. Geophys. Union 33, No. 6, 834-844.

Sverdrup, H. V. and W. H. Munk. 1947. Wind, sea,and swell: theory of relations for forecasting. U. S. Navy Hydrographic Office, Pub. No. 601.

Tick, J. L. 1959. A non-linear random model of gravity waves, 1. J. Math. and Mech. Vol. 8, No. 5, 643-652.

Yoshida,K. 1951. Energy distribution in the wind-wave spectrum. J. Oceano-graphic Soc. Japan, Vol. 7, No. 2, 49-54